BOLLETTINO DI GEOFISICA TEORICA ED APPLICATA VOL. XXXIII, N. 129 - MARCH 1991

L. PERUZZA (1), A. REBEZ (2), D. SLEJKO (2) and G. PADOAN (2)

WEIGHTED UNCERTAINTIES USED TO DETECT SEISMOGENIC STRUCTURES

Abstract. Some new parameters related to the earthquake hypocentral locations are defined. They are based on probabilistic criteria, and their behaviour offers a quantitative representation of the space distribution of the seismicity. They are the hypocentral probability (HP), that is the probability that at least one focus has occurred in the sample volume, the hypocentral density (HD), a simplified assessment of HP, and the energy density (ED), where energetic contents are introduced into the HD. A more unbiased interpretation of the earthquake data set is therefore possible. An application to the Friuli region outlines in detail some evidence previously only partly suggested by standard elaborations.

INTRODUCTION

Global geodynamic theories and knowledge of the Earth's interior have been greatly improved by the world-wide instrumental recording of earthquakes.

Considering that a predominantly brittle behaviour is invoked to explain the energy released by an earthquake, the ability to associate the seismicity with tectonic structures plays a fundamental role in geodynamic comprehension, especially for shallow seismicity (till 15-20 km depth). In fact, down to the first tens of kilometers, the pressure-temperature conditions and the composition of the earth's crust are empirically well constrained; in this way, the seismic activity can be regarded as an indicator of the actual stress conditions and discontinuities of the crust, and used in modelling the geodynamic behaviour of the region. Moreover, compared to other conditions, the shallow seismicity is the most dangerous, and the definition of seismogenic sources (i.e. the definition of where, when and how an earthquake has occurred, and could reasonably be expected in the future) is one of the first, fundamental steps in the seismic hazard assessment. This is particularly important in a country like Italy, where a complex geodynamic evolution exposes the majority of the territory to high seismic hazard, and where hypocentres are usually shallow.

Many disciplines contribute to correlating the seismicity to crustal heterogeneities or tectonic structures. The most common and simplest approach consists in the analysis of the earthquake distribution: epicentre maps (if possible in both segments, historical and instrumental, of an earthquake catalogue) define the seismic distribution in a horizontal plane, which can be very significant if vertical seismogenic faults do exist. However, even in this case, the alignment of epicentres can be biased by very high background seismicity in the region, or by bad locations of the quakes. If no vertical planes are expected (or more in general to verify the geometry of epicentre concentrations) vertical cross-sections of hypocentres are a good guide

Manuscript received November 15, 1990; accepted February 15, 1991.

1 C.N.R. Gruppo Nazionale Difesa Terremoti, Trieste, Italy.

2 Osservatorio Geofisico Sperimentale, Trieste, Italy.

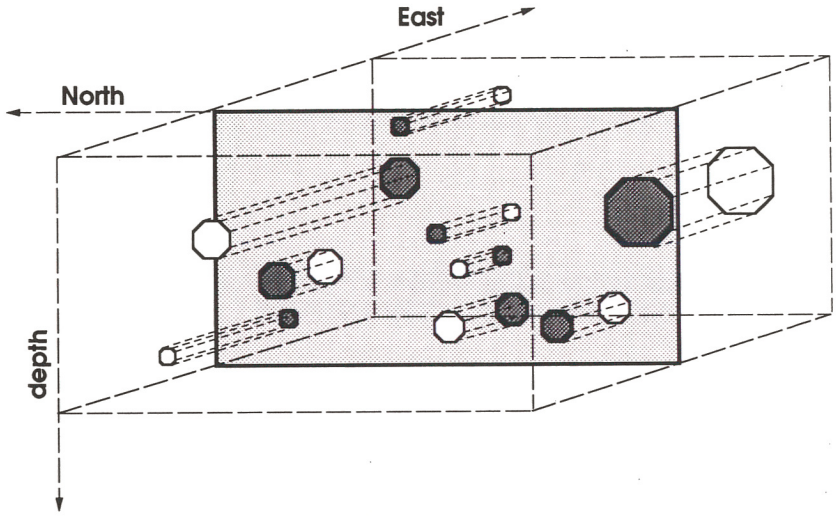

Fig. 1 - Projection of hypocentres onto a plane representing a vertical cross-section; the bold symbols are the projected earthquakes.

for interpreting the seismicity. The utilization of depth data automatically excludes the use of historical locations due to the large uncertainties in macroseismic determination. Usually, hypocentre vertical cross-sections plot the projection of the quakes located in a defined volume onto the median plane of the volume itself (Fig. 1); in this way, a vertical cross-section is defined by the coordinates of the extremes of the chosen profile and by a kilometric value giving the thickness of the prism to be projected. Obviously, the instrumental location of each quake is treated as a point to which a graphical representation of the magnitude, or of any other quantity representing the size of the event, can be associated. But this simplification is unacceptable, since the earthquake process has a finite volume and, moreover, the earthquake location is characterized by uncertainties. Even hypothesizing that hypocentres are not affected by errors, the geometrical interpretation of these pseudo-sections is not easy. In fact, the projection of a plane (idealized seismogenic structure) onto another is a line only when considering two infinitively thin planes, and is a strip if one (or both) of them has a finite thickness. If the position of a plane in space is defined by direction and inclination, the actual inclination of the projected plane is obtained only if the two planes are orthogonal in direction; surfaces of higher degree are more and more difficult to recognise in projection. Thus, the common use of hypocentre vertical cross-sections suggests the following operations:

- to trace profiles perpendicular to the expected structures;
- to use sections as thin as possible, so as not to "contaminate" differently oriented surfaces.

This means superimposing a priori knowledge on the seismogenic structure detection; this knowledge is usually derived from geological and geophysical data. Obviously, the inaccuracy of hypocentres could enhance different, unjustified interpretations. Moreover, the weight of each quake, given by the size of the symbol, does not clearly show the energy content.

The purpose of this study is to define an unbiased methodology for seismotectonic structure recognition which can quantify the concentrations of earthquakes approximately onto surfaces by taking into account the accuracy of the hypocentral location and weighting the energy released in the process. The first, incomplete formulation of this strategy has already been presented by Slejko et al. (1989b) and Peruzza et al. (1990a).

THE ERRORS IN EARTHQUAKE LOCATION

Let us assume that an earthquake catalogue is used to investigate the seismicity of a region.

The first obstacle to a correct recognition of active areas is the inaccuracy in the spatial focal parameters of the quakes. Usually, instrumentally computed hypocentres are considered reliable data with respect to the historically determined hypocentres (or more frequently epicentres); since the quality of the locations has increased with development in seismographic networks, they are widely used to present the earthquake distribution over time-windows, representing different ranges of reliability in the hypocentral coordinates. In this way, the more recent the definition of the seismicity, the less scattered and imprecise is considered the earthquake distribution.

Taking into account only the instrumental segment of the earthquake catalogue, the statistical parameters associated with the solutions can be used to evaluate the location accuracy of each event. It is true that the standard errors may not represent actual limits to the earthquake location; an inadequate earth velocity model, an uneven geometrical distribution of the recording stations, or systematic and random reading errors may influence not only the solution of the location but even its statistical interpretation.

Most of the earthquake location procedures give the solution by solving a system of equations where the difference between the computed and the observed arrival times is minimized, giving the computation of the residuals on the arrival-time at the stations and of the statistical parameters of the four unknowns (latitude, longitude, depth, and origin time). The meaning of the computed errors varies in the different regional earthquake location codes but the basic, common assumption is that statistical treatment evaluates only the effect of random reading errors on the arrival time, which are assumed to be normally distributed with zero mean and σ standard deviation. The diagonal elements of the inverse matrix of the coefficients of the unknowns, being related to the time residuals, enable one to obtain the standard errors in longitude, latitude, depth and origin time; however, the error limits are approximate since they are based on a linearization of a non-linear system. Some programs output the maximum range of the stability of the solution (for example Hypo 71: Lee and Lahr, 1975); others give the errors related to a confidence region in the solution (Hypoellipse: Lahr, 1979).

Knowing the meaning of the output location errors, it seems obvious to associate an error-dependent volume to an earthquake hypocenter: this concept has to be kept physically well distinct from that of the finite dimension of the earthquake source.

Let us consider an experiment consisting in occurring an earthquake somewhere in the earth. Its hypocentral location is the elementary event associated with the experiment, the event belonging to the sample space given by all points in the earth which are possible hypocentres of a quake.

PROBABILISTIC QUANTITIES ASSOCIATED WITH EARTHQUAKE LOCATIONS

Elementary Probability

Let X (longitude), Y (latitude) and Z (depth) be three independent random variables associated with a hypocentre in the sample space; for each value of the random variable, it is possible to define a probability value. Let us hypothesize that the location program gives the mean hypocentral position and the standard deviations on three principal axes, assuming a normal distribution of errors.

Therefore, the longitude X can be considered as a continuous random variable and its probability density function (PDF) is given by

$$f_X(x) = \frac{1}{\sigma\sqrt{2\pi}} e^{\frac{-(x-\mu)^2}{2\sigma^2}} \tag{1}$$

where μ is the mean value and σ the standard deviation. Eqn.(1) applies similarly to the random variables Y and Z.

The probability that the random variable X will assume a value in the interval (a, b) is

given by the integral

$$P\ (a<X\leqslant b)=\int_a^b f_X(x)dx, \tag{2}$$

and it corresponds to the area situated between the density curve and the horizontal axis between the points with coordinates (a, $f_X(a)$), (b, $f_X(b)$).

The probability of the joint occurrence of X, Y, and Z in some region of the sample space is determined by integration of the joint PDF over that region.

For example,

$$P\ [(x_1<X\leqslant x_2),\ (y_1<Y\leqslant y_2),\ (z_1<Z\leqslant z_2)]=\int_{x1}^{x2}\int_{y1}^{y2}\int_{z1}^{z2} f_{X,Y,Z}\ (x,y,z)\ dx\ dy\ dz \tag{3}$$

but

$$f_{X,Y,Z}\ (x,\ y,\ z)\ =\ f_X(x)\ f_Y(y)\ f_Z(z)$$

if the random variables are stochastically independent, where $f_X\ (x)$, $f_Y\ (y)$, $f_Z\ (z)$ indicate the marginal distribution of X, Y, and Z. So, the integration can be symplified to

$$EP=P\ [(x_1<X\leqslant x_2),\ (y_1<Y\leqslant y_2),\ (z_1<Z\leqslant z_2)]=\int_{x1}^{x2} f_X(x)dx\int_{y1}^{y2} f_Y(y)dy\int_{z1}^{z2} f_Z(z)dz. \tag{3b}$$

In this way, given the location of an earthquake, the probability, here defined as *Elementary Probability (EP)*, that its hypocenter is located inside an elementary volume of the earth, is given by the product of the related probabilities along the three axes: *EP* is, therefore, a

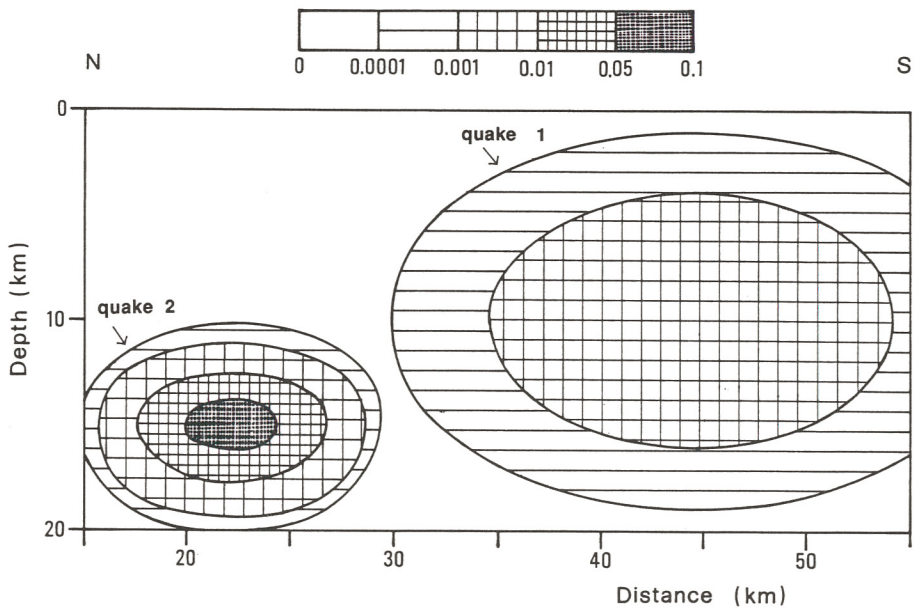

Fig. 2 - *EP* distribution of two synthetic earthquakes along a vertical cross-section (see their focal parameters in the Table).

function of the spatial coordinates.

The integration, assuming a normal distribution for the variables, can be limited to the interval $(\mu-3\sigma, \mu+3\sigma)$ for each independent variable without a significant loss of probability: that is to say, a volume centred on the mean value of a hypocentral solution (μ_X, μ_Y, μ_Z) with dimension $6\sigma_X \cdot 6\sigma_Y \cdot 6\sigma_Z$ has probability 0.991922 of having been the "real" hypocenter of the given earthquake.

Obviously other PDF's than eqn. (1) could be used to define *EP*, in relation to the statistical characteristics of the errors defined by the location program. In any case, this treatment distributes the hypocenter, originally represented by a point, over a non-uniform volume.

In Fig. 2 the different *EP* distributions of two synthetic earthquakes (see the focal parameters in the Table) are given along a section. The plane of the section has been meshed by 2 km wide squares and the thickness of the section itself is taken as 2 km: this creates a series of small cubes where the *EP* is computed; unlike in Fig.1, only a part of the earthquake is counted in this way. The error dependency of the *EP* distribution is evident. Here, small standard errors make the *EP* of quake 2 more concentrated. The single event treated in this way does not improve the seismic comprehension of the study area: a relevant improvement is given by the analysis of a set of data. So, given a sample volume inside the earth (or, in particular, inside the crust), and defining as *Elementary Probability* EP_i the probability that the i-th earthquake of the catalogue has its hypocenter located inside that space, some new quantities, which will now be introduced, describe the seismogenic characteristics of the volume.

Table — Hypocentral parameters of the quakes of Fig. 2.

quake	lat (°)	lon (°)	erh (km)	dep (km)	erz (km)
1	46.1	13.0	5.0	10.0	3.0
2	46.3	13.0	2.0	15.0	1.0

Hypocentral Probability

Theory

Let us define *Hypocentral Probability (HP)* as the probability that at least one event of a given catalogue has its hypocenter located inside a chosen volume in a given period of time. Let A and B denote two earthquakes, each of which may or may not have occurred in the sample volume. The events A and B are characterized by the probability of success EP_A and EP_B *(Elementary Probability:* occurrence of the earthquake in that particular volume), where these values derive from the random variables X, Y, and Z associated with the hypocenter. The compound event, which consists in the occurrence of at least one of the two independent events A and B, has the related probability $HP_{[2]}$ given by (Papoulis, 1977)

$$HP_{[2]}=P(A\cup B) \equiv P(A+B)=P(A)+P(B)-P(A\cap B)=P(A)+P(B)-P(A)P(B)= \\ =EP_A+EP_B-EP_AEP_B. \tag{4}$$

From the general addition rule for an arbitrary number m of A_i events, $HP_{[m]}$ is obtained in the following form (Cramer, 1955)

$$HP_{[m]}=P(A_1+A_2+A_3+\ldots+A_m)=P(A_1)+P(A_2)+\ldots+P(A_m)-P(A_1A_2)-P(A_1A_3)-\ldots$$

$$\ldots-P(A_{m-1}A_m)+P(A_1A_2A_3)+P(A_1A_2A_4)+\ldots+P(A_{m-2}A_{m-1}A_m)-\ldots+(-1)^{m-1}P(A_1A_2\ldots A_m)=$$

$$=\sum P(A_i)-\sum P(A_iA_j)+\sum P(A_iA_jA_k)-\ldots+(-1)^{m-1}P(A_1A_2\ldots A_m). \tag{5}$$

If each A_i event is characterized (as in the previous case of two earthquakes) by probabi-

lity of success EP_i, eqn. (5) can be expressed as

$$HP_{[m]} = \sum_{i} EP_i - \sum_{i,j} EP_iEP_j + \sum_{i,j,k} EP_iEP_jEP_k - \ldots + (-1)^{m-1} EP_1EP_2 \ldots EP_m, \quad (6)$$

where the first term is the sum of the EP_i's, the second the sum of all combinations of two events, the third of three events, and so on.

The computation of *HP* becomes extremely onerous when the number of earthquakes increases. In fact no truncation of eqn. (6) is possible because, although each single EP_i is a number smaller than 1, and thus the product of many *EP* 's causes an exponential decrease in the weight of the higher terms, the factorial increase in the number of terms for couples, triplets, etc., makes their contributions significant.

Eqn. (6) cannot be analytically studied: here a simplified approach to its principal properties is proposed.

For example, let us consider a fixed probability of success $EP=0.2$ associated with each event; this case could be considered a sequence of simple Bernoulli trials, with the outcomes of the experiments mutually independent and with unchanged probability of success. Calling S the random number of successes, the probability of at least one success in two trials, according to eqn. (6), is given by

$$P(S \geq 1) = HP_{[2]} = EP_A + EP_B - EP_AEP_B = 2\,EP - EP^2 = 0.4 - 0.04 = 0.36. \quad (7)$$

If 5 trials are considered, eqn. (6) becomes

$$HP_{[5]} = \binom{5}{1} EP - \binom{5}{2} EP^2 + \binom{5}{3} EP^3 - \binom{5}{4} EP^4 + \binom{5}{5} EP^5 = \\ = 5\,EP - 10\,EP^2 + 10\,EP^3 - 5\,EP^4 + EP^5, \quad (8)$$

and with 10 trials the sum has to be extented to the 10th term:

$$HP_{[10]} = \binom{10}{1} EP - \binom{10}{2} EP^2 + \binom{10}{3} EP^3 - \ldots + \binom{10}{9} EP^9 - \binom{10}{10} EP^{10}, \\ HP_{[10]} = 10\,EP - 45\,EP^2 + 120\,EP^3 - 210\,EP^4 + 252\,EP^5 - \ldots + EP^{10}, \quad (9)$$

where the rapid increase in the number of factors is clear.

Plotting *HP* versus increasing order of computation of the formula (Fig. 3), an oscillatory behaviour of the function is seen, with oscillations neither symmetric nor asymtotic to the true value (which is reached upon complete development of the formula), and amplitude of the oscillations dependent on the number of trials as well as on the *EP* value of success. Fig. 3 gives a schematic representation of 4 different cases with 2 (Fig. 3a), 5 (Fig. 3a), 10 (Fig. 3b) and 100 (Fig. 3c) trials; it can be seen that while in the first three cases the function directly converges to the true value, with many trials (or with high *EP* values) the function has increasing amplitude oscillations at the beginning, and the convergence occurs only with the inclusion of the final terms in the formula.

The situation is made more complicated by the fact that the *EP's* are not constant but variable, being computed from the random variables X, Y, and Z associated with each hypocenter.

These observations show that a complete resolution of eqn. (6) is necessary to obtain the actual *HP* value.

Calculation

A Fortran program has been designed to perform the computation of *EP* and *HP* values

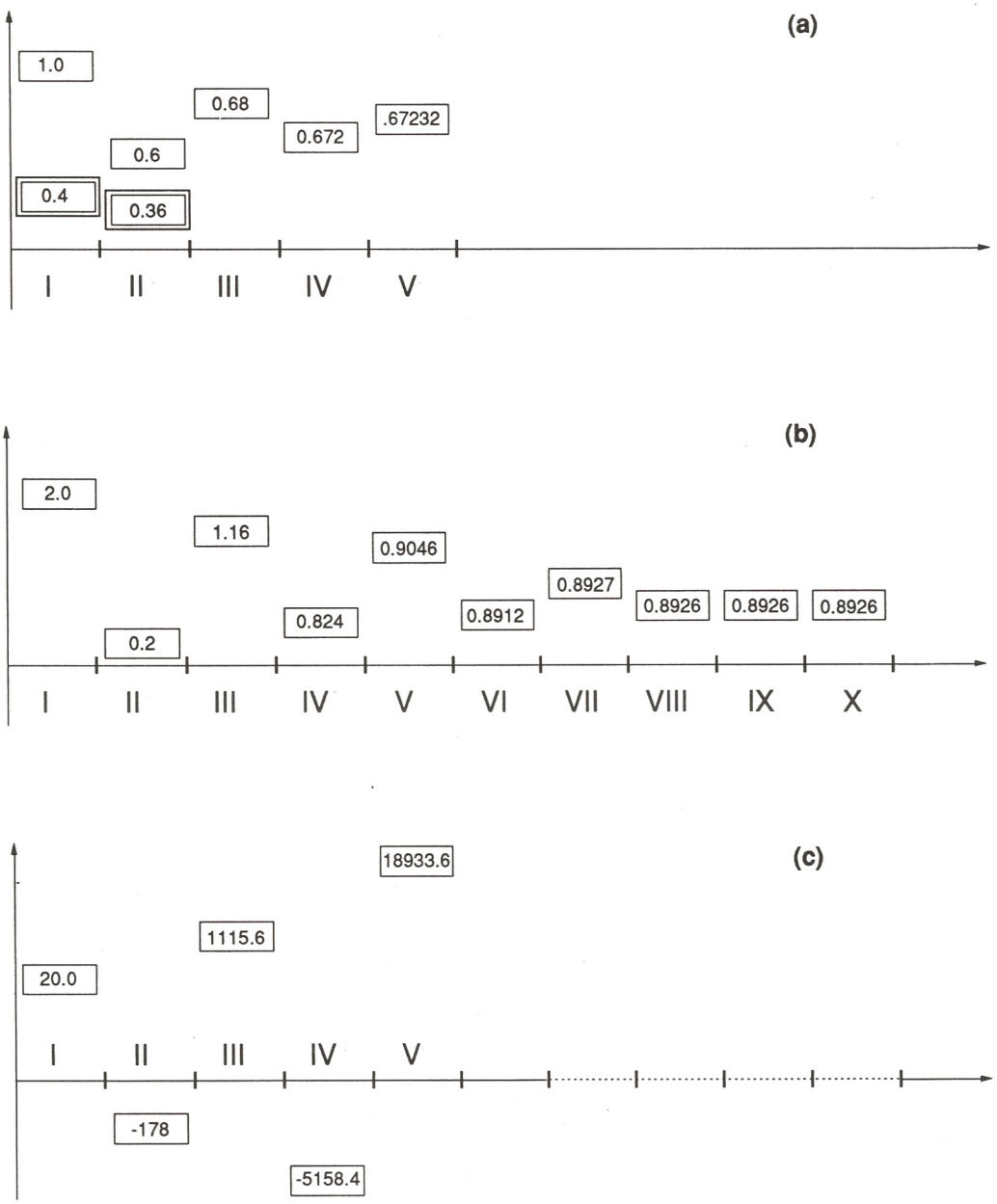

Fig. 3 - Behaviour of the *HP* value as function of the development of eqn. (6); (a) refers to the occurrence of 2 (double frame) and 5 events, (b) to 10, and in (c) there are only the first steps for 100 earthquakes.

in a set of small sample volumes lying on a plane. An *HP* map can be produced, and it is thus possible to go beyond the classical representations of seismicity by epicentral maps and cross-sections of hypocentres. Given a set of earthquakes, the *Elementary Probability* EP_i in a sample volume can be easily computed from eqns. (1) and (4); the coordinates of the processed cell represent the limits of the integral (usually solved by routine mathematical functions) which in any case do not have to exceed the interval $(\mu-3\sigma, \mu+3\sigma)$ for each axis. When the m *EP* values are assessed, the automatic *HP* computation routine has three tasks:

1) to recognize and address all and only the (unrepeated) combinations of eqn. (5) to com-

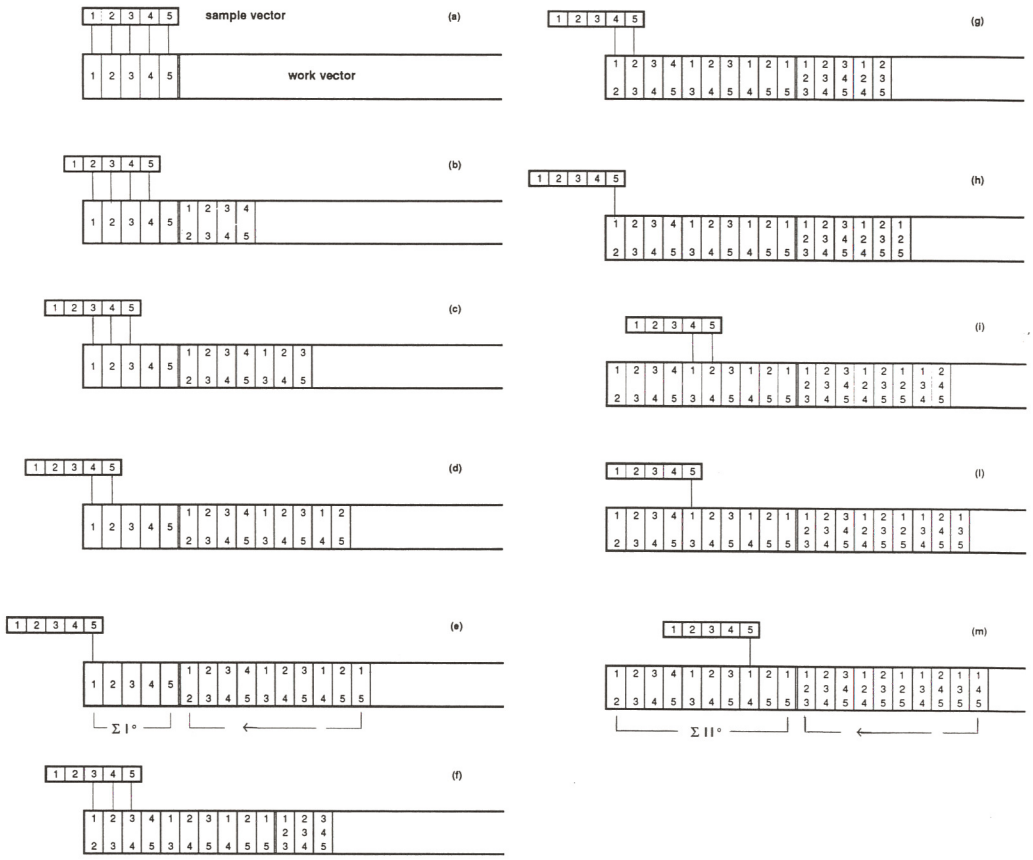

Fig. 4 - Scheme for the recognition and computation of the elements of eqn. (6) in the simple case of 5 trials. The numbers from 1 to 5 identify the values of *EP* associated with each event. In (a) a work vector, where the first order terms are collected, is generated by the sample vector. From (b) to (e) the computation of the second order terms is illustrated; a relevant shifting of the sample vector makes the recognition of all the unrepeated products possible. At the end of the computation of one cycle of products (e), the sum is taken over the useless elements and the work vector is reorganized (f); then a new cycle starts. From (f) to (m) the computation of third order terms is done and the process repeated.

pute the products;

2) to take care of computer precision (critical when values are too small or too big) when assessing the *HP*;

3) to optimize the memory utilization.

The problems have been solved with a series of nested loops operating as in the scheme of Fig. 4. The sample vector generates a work vector (Fig. 4a) in which the terms of subsequent order are progressively computed by the relevant shifting of the sample vector (from Fig. 4b to e). Then, the sum of the terms of first order is made and kept in memory to adjust the position of the following terms and to restart with a new cycle (from Fig. 4f to m); the number of repetitions of the loops is equal to the number of samples.

The dimension of the work vector grows dramatically with the number of samples; this is the reason why the reordering of each cycle is not sufficient. With only 50 earthquakes, the dimension of the work vector reaches $2.4796 \cdot 10^{14}$ elements, hardly manageable even with a large computer, considering also the high precision needed for the variables.

Application of the associative property to the sum of the events makes the computation possible. In fact

$$P(A \cup B \cup C) \equiv P(A+B+C) = \\ = P(A)+P(B)+P(C)-P(A \cap B)-P(A \cap C)-P(B \cap C)+P(A \cap B \cap C), \tag{10}$$

and

$$P(A+B+C)=P((A+B)+C)=P(A+B)+P(C)-P((A+B) \cap C), \tag{11}$$

which is the easiest way to compute eqn. (6) because the probability of a single event can be substituted by the probability of a group of events. In this way, the limit of the event number, with the relative problems of dimensioning and memory optimization, can be bypassed according to hardware characteristics.

In conclusion, the computation of an *HP* map can be performed in the following four steps:

I - defining the characteristics of the section (if a vertical plane, the coordinates of the extremes, the thickness, usually a few kilometers to obtain a good resolution, and the gridding; for a horizontal plane, the coordinates of opposite vertices, depth level, thickness and gridding);

II - defining the database of earthquake locations (filtering is possible on time interval, error range, or magnitude range, depending on the objectives);

III - computing for each elementary cell the *EP*'s of each event and then computing the *HP* value as in eqn. (6);

IV - interpolating the *HP* values obtained for each cell.

The gridding of the plane has consequences for the contouring procedures and run time; the dimension of the mesh has to be carefully chosen with regard to the data base of earthquake locations.

Hypocenter Density

Given a database of earthquake locations and a prismatic cell inside the earth, the method of computing the *EP* for each event has been described.

The sum

$$HD_{cell} = \sum_{i=1}^{N} (EP_i)_{cell} \tag{12}$$

is here defined as *Hypocenter Density (HD)*, with N the number of events for which an *EP* value is defined in the cell. It represents the truncation after the first term of eqn. (6) and is useful for many purposes.

First of all, it represents a sort of count of the number of earthquakes located in that cell; in fact, the *EP* of an earthquake in a cell can be considered the fraction of one event falling in that volume, assuming a normal distribution of the location errors. Then, its value is almost the same as the *HP* when there are few events in a cell, especially if the related *EP* is very small. But what is even more important is that the shape of an *HD* contour map is very similar to an *HP* map, even if the quantity *HD* cannot be considered a probability, and the range of its values is different (it can exceed 1). Finally, computation of the *HD* allows a great time saving compared to *HP*, which is very important in the initial phases of the work.

Energy Density

Energy can be introduced into the analysis to include the magnitude of the earthquakes. In fact, it is clear that no importance is given to the strength of an event in either the *HP* or the *HD* formulations. A small event with small standard errors could weigh more than a bigger one with greater errors, which is not completely acceptable for interpretation.

So it is useful to introduce the *Energy Density (ED)* given by

$$ED_{cell} = \sum_{i=1}^{N} (EP_i \, W_i)_{cell}, \tag{13}$$

where W is a quantity related to the energy released by each earthquake. Sometimes the dynamic range in terms of energy between a strong earthquake and a weak one turns out to be too large and it is useful to introduce a smoothing factor to reduce the difference: in this case, a quantity such as the tectonic flux can be invoked.

Many authors have proposed relationships for converting magnitude into energy; here a detailed analysis is not given, since different assessments of W have to be justified in relation to the data set and the objectives of the work. For example, other quantities such as the seismic moment or the macroseismic intensity can be useful in some cases.

CAPABILITY OF THE METHOD

The capabilities of the previously described methodology and the meaning of the different representations of *HP*, *HD* and *ED* maps can be separated into:

- intrinsic capacities of the method;
- applications in the field of seismogenesis.

In the first class, the principal characteristic of the method is to represent the seismicity in terms of absolute quantities, if a unit of time and space is taken into account. This effect of scaling the seismicity makes the *HP*, *HD* and *ED* maps an effective way to present and compare the seismicity of different regions; it is a better way of representation than the old, commonly used parameters like, for example, seismic activity (Riznichenko, 1959) because of the inclusion of the uncertainties in earthquake location.

The different information contents of *HD* and *ED* maps can lead to the recognition of homogeneous regions in terms of epicenter distribution and energy release.

Another intrinsic characteristic of the method is to consider the effect of location uncertainties; an example of the different scattering due to errors in location has been already given in Fig. 2. The effect of the increasing quality of the earthquake catalogue is presented in Fig. 5 for two vertical *HP* sections (details on location are given in the following paragraph). Fig. 5a and b was obtained using all the locations reported in the catalogue, while a low-pass filter on errors (of 2 km horizontally and 3 km vertically) has been used to produce Fig. 5 c and d; even if the two sections (Section 2 and Section 5, respectively, in the following) are affected by very different levels of activity, the image of the seismicity is nearly the same using all the earthquakes of our catalogue or only the best located. This makes the representation of the seismicity independent of an a priori choice of what "good data" means, and all the information weighted by the formulation of eqn. (1) is taken into account.

Considering applications, the problems of projective geometry and of point sources presented in the introduction are bypassed with this method. Since each earthquake has an associated probabilistic volume, sections and maps can be constructed with high precision, making seismogenic recognition of structures easy. In addition, the geometry of the active faults is not the result of an individual interpretation of alignments and concentrations of points; dense gridding and good contouring ensure geometry control.

Another important aspect for seismogenesis is the possibility of time evolution analysis. Fig. 6 illustrates the variation of *HP* values in time on a section; different geometries involve either the background seismicity (Fig. 6a and b) or a particular seismic sequence (Fig. 6c). The time windows here used were adjusted with the help of a strain release versus time graph, and considering samples with the same slope to be homogeneous.

APPLICATION TO THE FRIULI AREA

The new method was applied to the Friuli area (northeastern Italy, Fig. 7), a seismic region

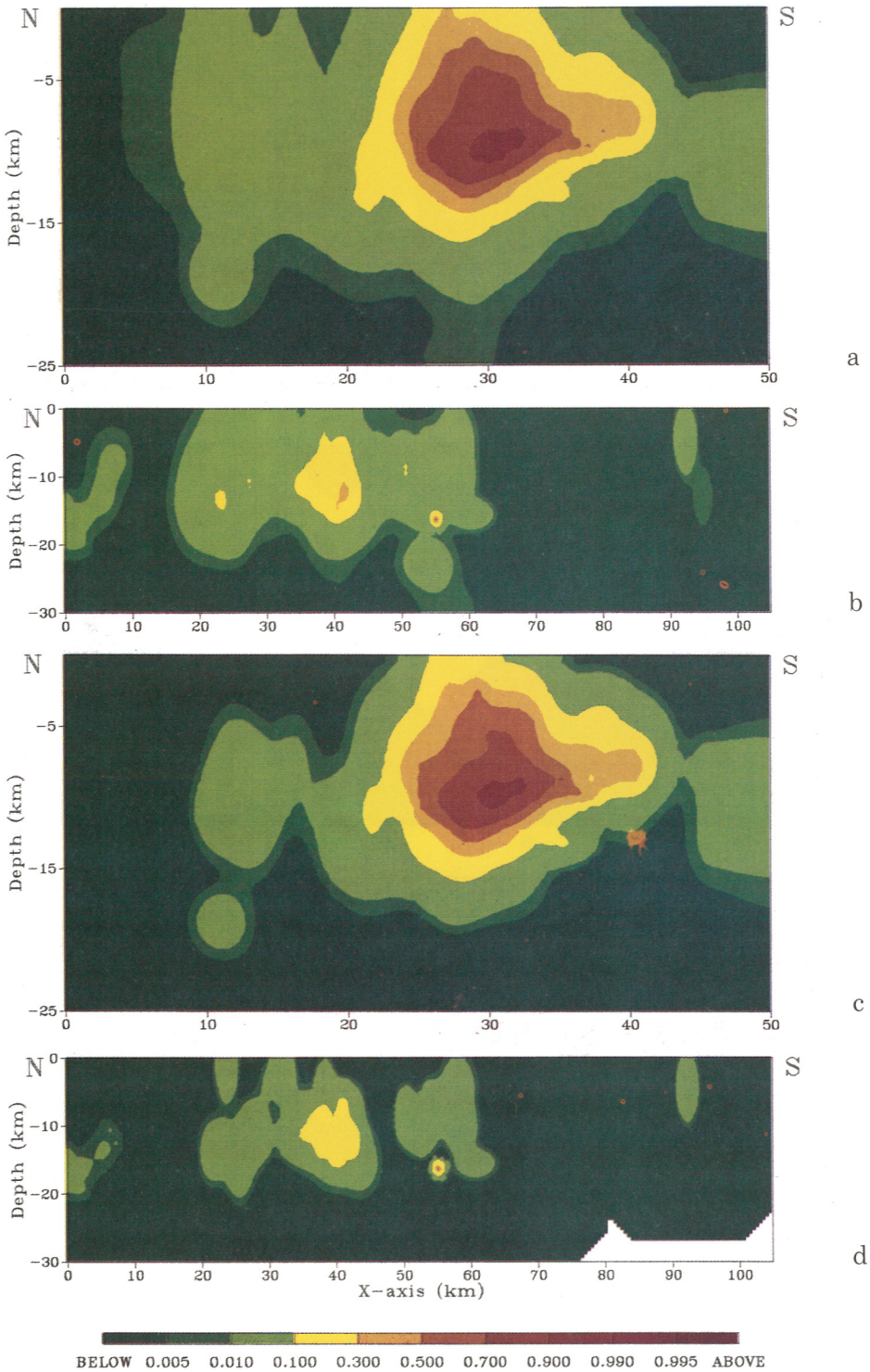

Fig. 5 - Maps of *HP* for two sections (Section 2 and Section 5): a and b) obtained using all the locations of the earthquake catalogue (OGS, 1977-1981,1982-1989); c and d) obtained using the locations with horizontal error less than 2 km and vertical error less than 3 km.

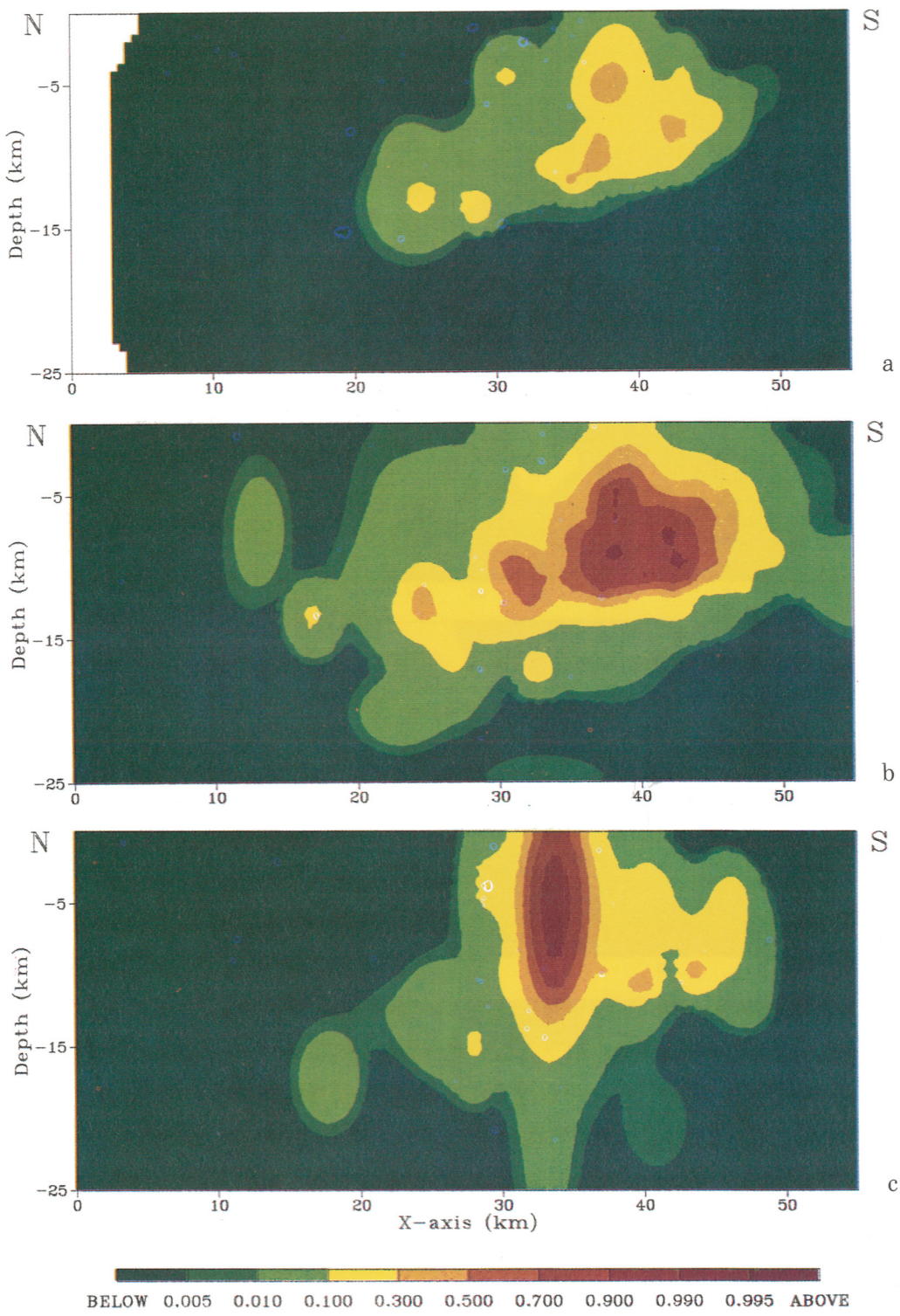

Fig. 6 - Maps of *HP* to demonstrate the capabilities of the method in a time evolution analysis of a section (in the following referred as Section 3); (a) is obtained with the locations from 1977 to 1979; (b) from 1980 to 1986; (c) from 1987 to March 1989. The style for the last period is very different.

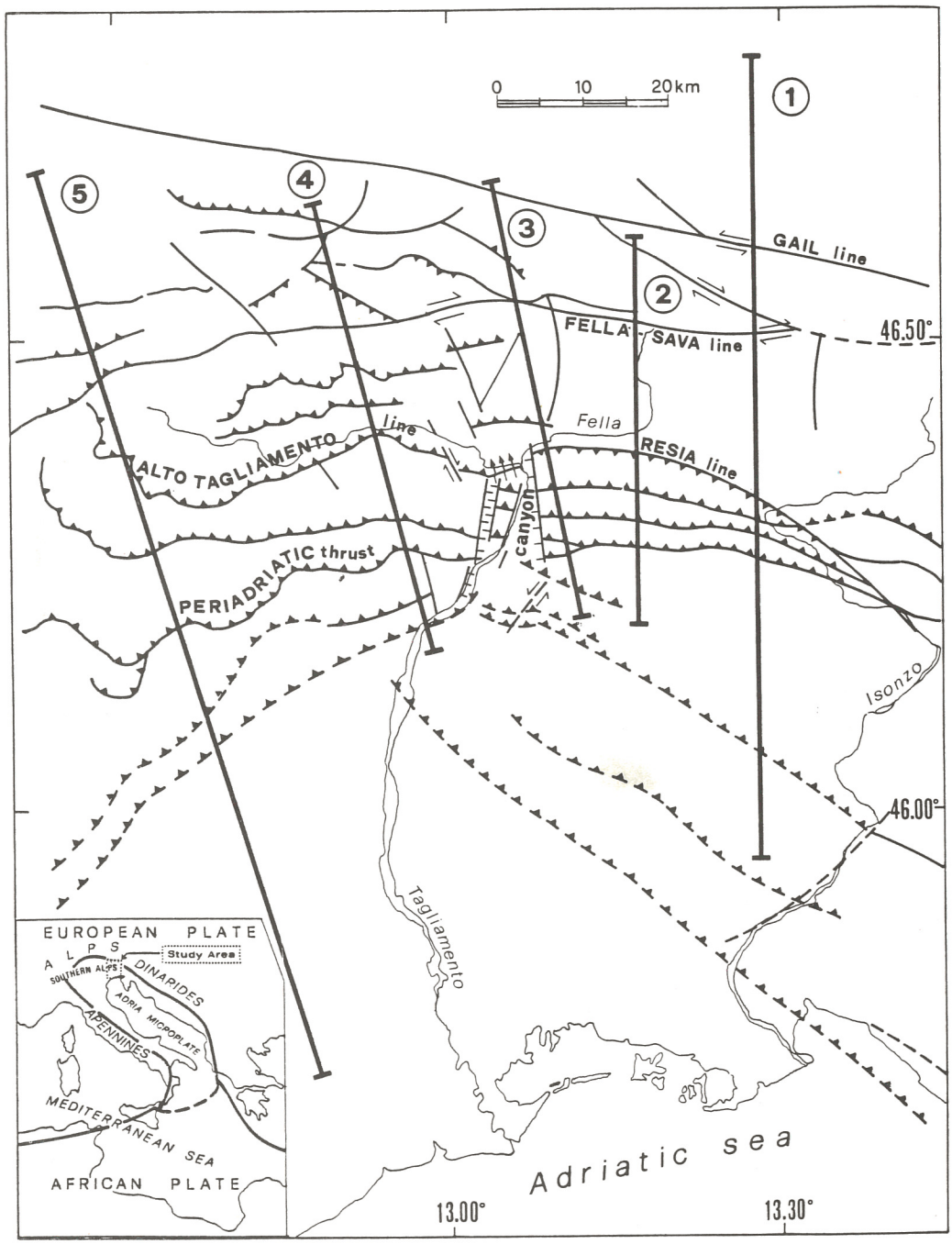

Fig. 7 - Tectonic map of Friuli (modified from Carulli et al., 1982 and Slejko et al., 1989a): saw-toothed line = thrust, hatched line = normal fault, hatched line with arrows = reverse fault; line with parallel arrows = strike-slip fault; and location of the studied sections. The sections presented in this study are numered from 1 to 5 moving from east to west. The main tectonic elements are indicated.

intensively studied after the 6.4 magnitude earthquake of May 6, 1976. Since 1977, a local seismometric network managed by the Osservatorio Geofisico Sperimentale of Trieste (OGS) has been recording the local seismicity, locating (Lee and Lahr, 1975) up to March 1989 about 6500 shocks in the magnitude range 1.5-5.2 (OGS, 1977-1981, 1982-1989).

In Figs. 8 to 12, five vertical sections, already shown and interpreted in Slejko et al. (1987, 1989a), are presented again to compare with the level of information and detail now reached. The sections are nearly all N-S oriented (north always on the left side of the figures) and they are presented from east to west; the locations of the sections are given in Fig. 7 with the main tectonic elements.

In the classical vertical cross-sections (marked in Figs. 8 to 12 by (a)), the hypocenters are represented by a circle centred on the coordinates of the location and with radius proportional to the magnitude. The thickness of the sections has been enlarged with respect to the sections already published (Slejko et al., 1987, 1989a) to contain all the events contributing to the new maps. To evidence the distance of the mean position of the hypocenters from the projection plane, symbols are plotted in different colours (blue when the distance is greater than the half thickness of the section, red otherwise).

HP maps (sigled by (b)) represent the occurrence probability distribution of at least one earthquake. *HD* maps are not shown here, since they give very similar information to *HP* maps: their main use is, as already noted, during the analytical phases of the work.

In *ED* maps (identified by (c)), the parameter W of eqn. (13) used in this computation is defined as the energy obtained from the local magnitude with the Richter (1958) relationship.

For both the *ED* and *HP* maps, a square mesh one kilometer wide is considered, while the thickness of the section is taken as 2 km (with the exception of Section 5 which is 10 km wide due to lower density of foci).

The details of each section are quite different and the geometries involved are represented in an extremely clear manner.

The classical representation of Section 1 (Fig. 8a and Fig. 10 in Slejko et al., 1989a) shows a maximum density of foci very gently dipping to the north at about 10 km depth and very surficial hypocentres with possible antithetic orientation. Considering *HP* (Fig. 8b), two trends are seen; an elongated maximum of hypocentral probability is dipping northwards (from 6 to 14 km depth) with low inclination; it is surrounded by an almost circular area of intermediate (0.5) probability that reaches the surface in the Val Resia - Monti Musi zone, at 50 km on the x-axis, where some north-verging structures (e.g. the Resia thrust) are considered to be neotectonically active. Further north, a channel of low (less than 0.1) *HP* separates another nearly vertical zone deepening southwards. The scenario is quite different when the *ED* map is considered (Fig. 8c); here the more important *HP* maximum appears as two small peaks (between 50 and 60 km on X) while the low-probability channel is replaced by the most important circular area of high *ED* which refers to a 4.8 magnitude quake. This is a case of discrepancy between the main seismicity distribution and the maximum energy release.

The main evidence shown by Section 2 in the classical representation (Fig. 9a and Fig. 11 in Slejko et al., 1989a) is the northward vertical alignment of foci under a well known strike-slip fault (Fella-Sava line). The *HP* distribution of Section 2 (Fig. 9b) shows a very similar behaviour to Section 1, but with an increasing importance of the subhorizontal, northward dipping structure (shown by the areas of up to 0.3 probability) compared to the vertical one. The *HP* and the *ED* representations are quite similar in general trend since the limit of the northernmost activity is clearly defined by the *ED* map (Fig. 9c) and the geometry of the subhorizontal structure is evidenced. In addition, a more surficial energy peak at 25 km on the X-axis from the northern corner refers to a stronger (magnitude 4.5) earthquake.

Two northward dipping alignments of foci, related to two important tectonic lines, are evidenced by the classical representation of the seismicity in Section 3 (Fig. 10a and Fig. 12 in Slejko et al., 1989a). In addition, the main focal depth seems to increase moving westwards. The updated version of the section (Fig. 10a) shows, moreover, the notable seismic crisis of February 1988, mainly located in the Monte Amariana zone (north of the Tagliamento canyon),

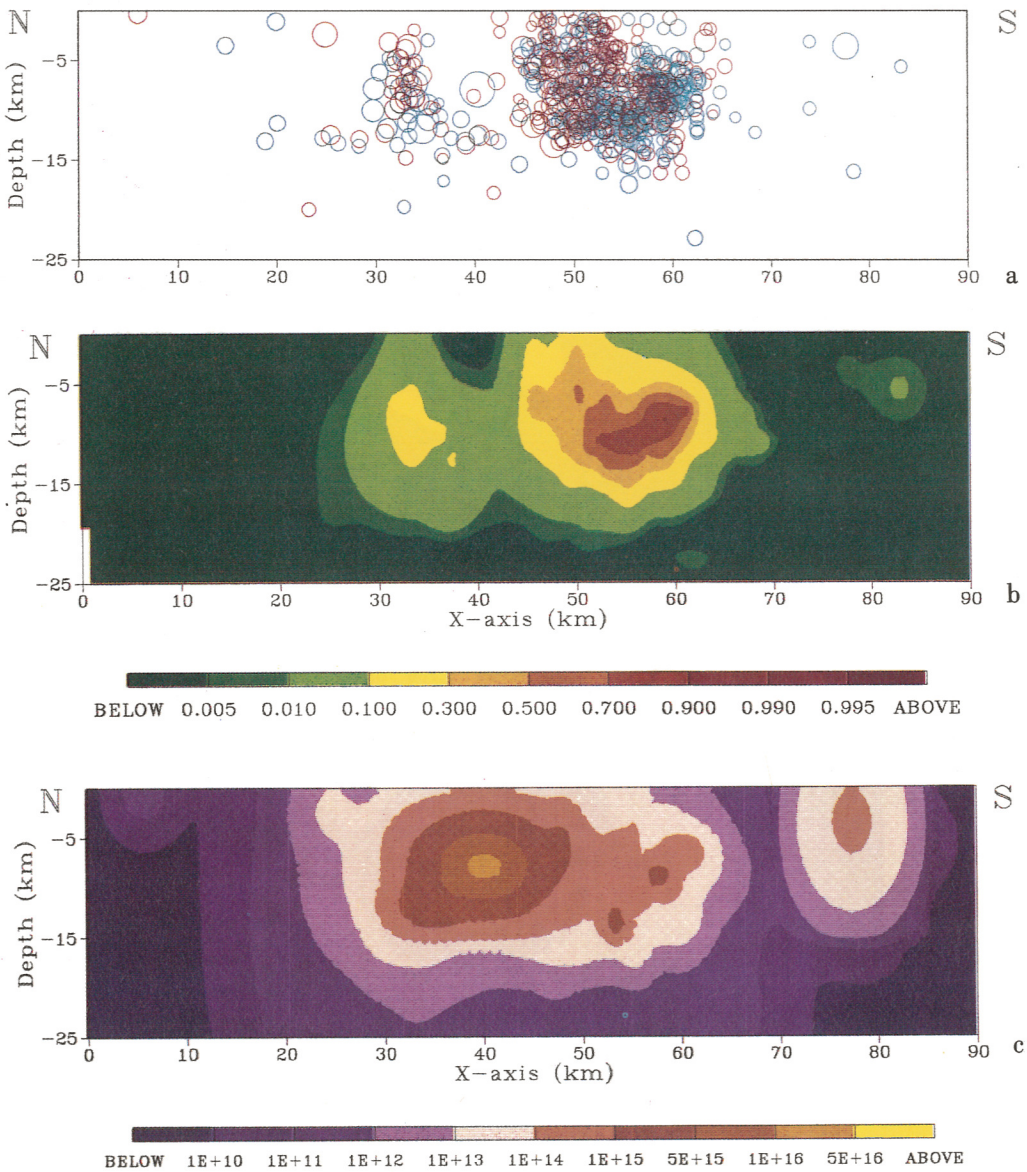

Fig. 8 - Maps of classical cross-section (a), *HP* distribution (b), and *ED* distribution (c) for Section 1. The coordinates of the extremes are 13.28 E - 46.80 N (the left corner), 13.28 E- 45.94 N (the right).

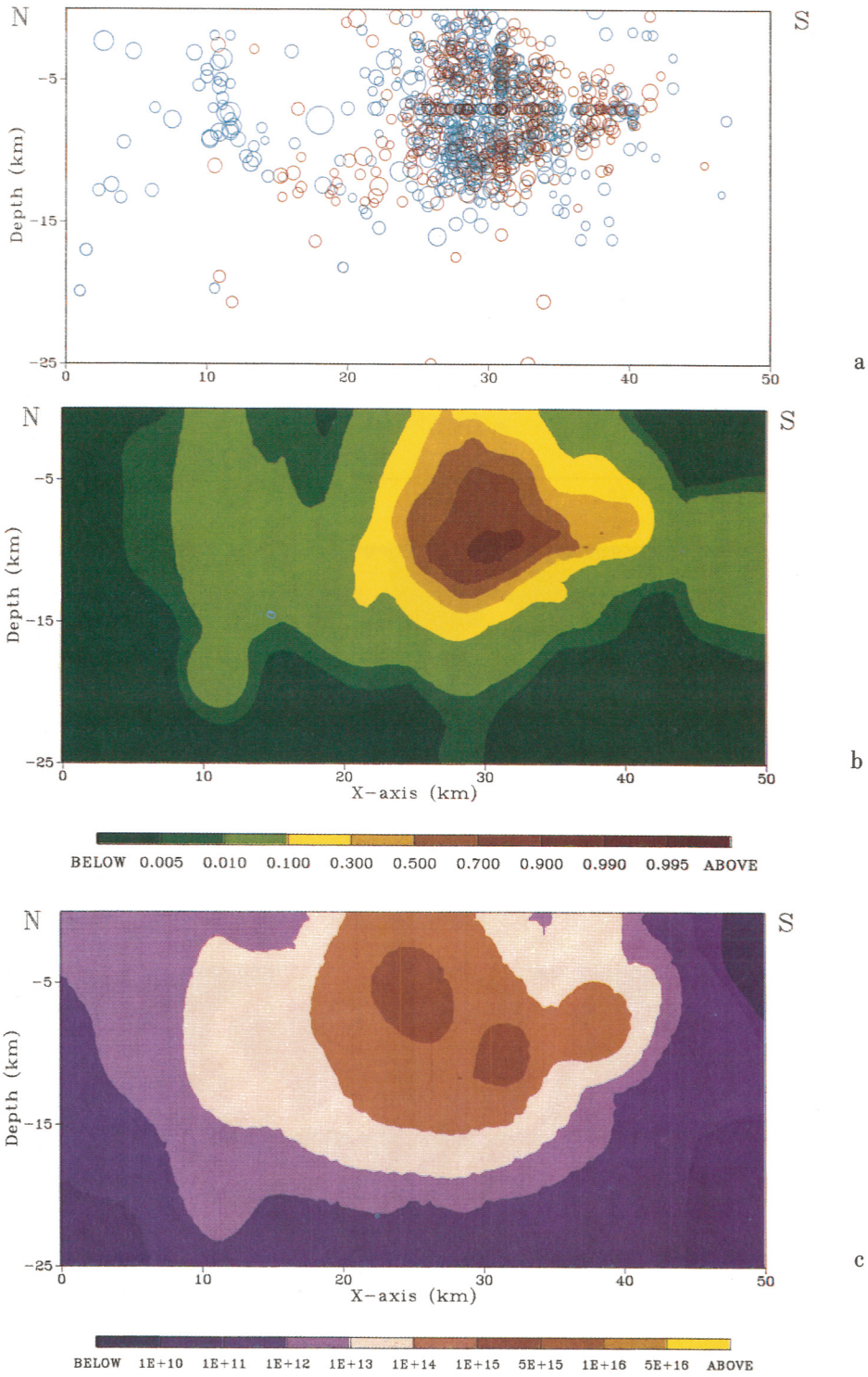

Fig. 9 - Maps of classical cross-section (a), *HP* distribution (b), and *ED* distribution (c) for Section 2. The coordinates of the extremes are 13.17 E - 46.60 N (the left corner), 13.17 E- 46.19 N (the right).

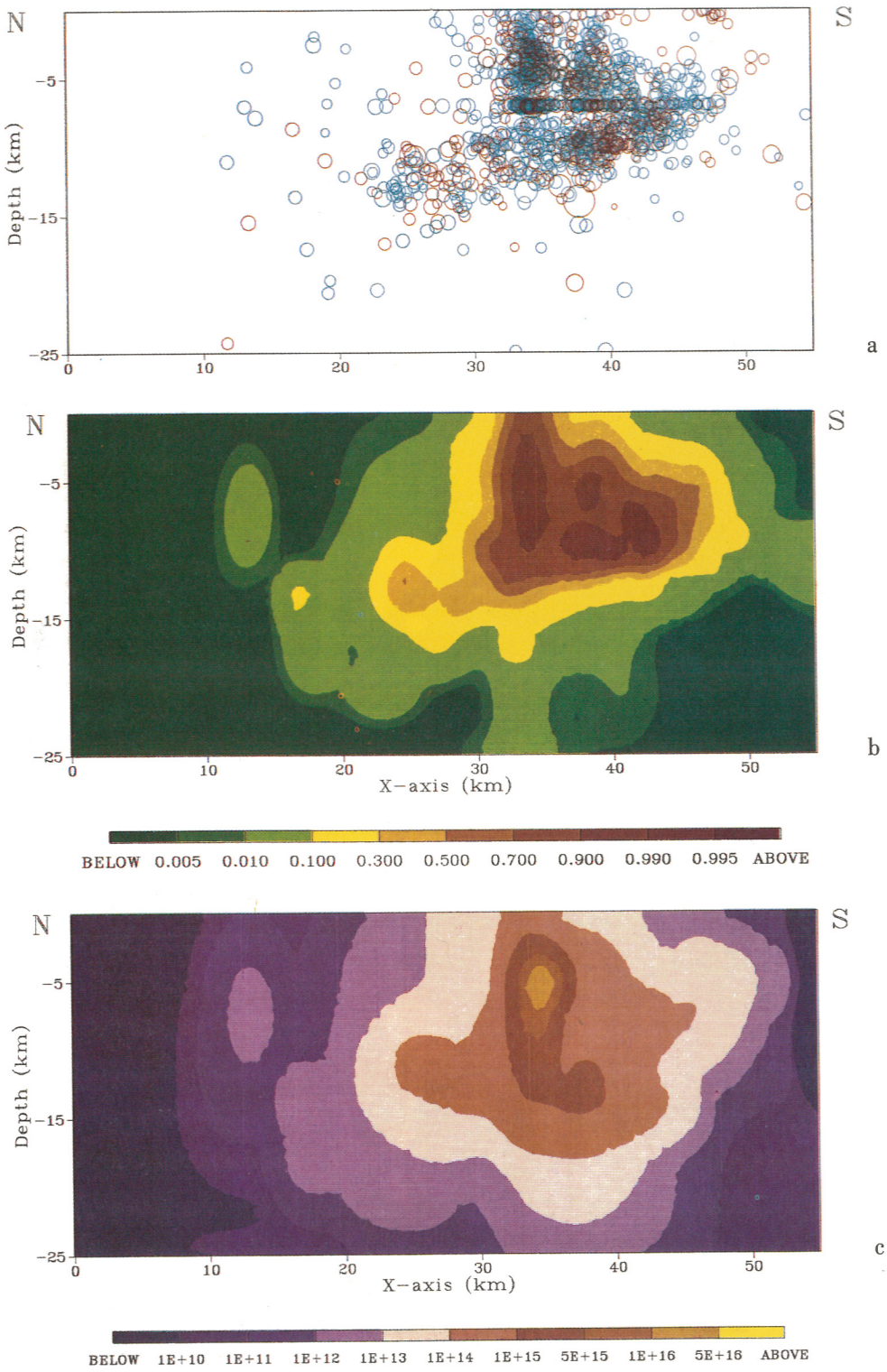

Fig. 10 - Maps of classical cross-section (a), *HP* distribution (b), and *ED* distribution (c) for Section 3. The coordinates of the extremes are 13.04 E - 46.66 N (the left corner), 13.12 E - 46.20 N (the right).

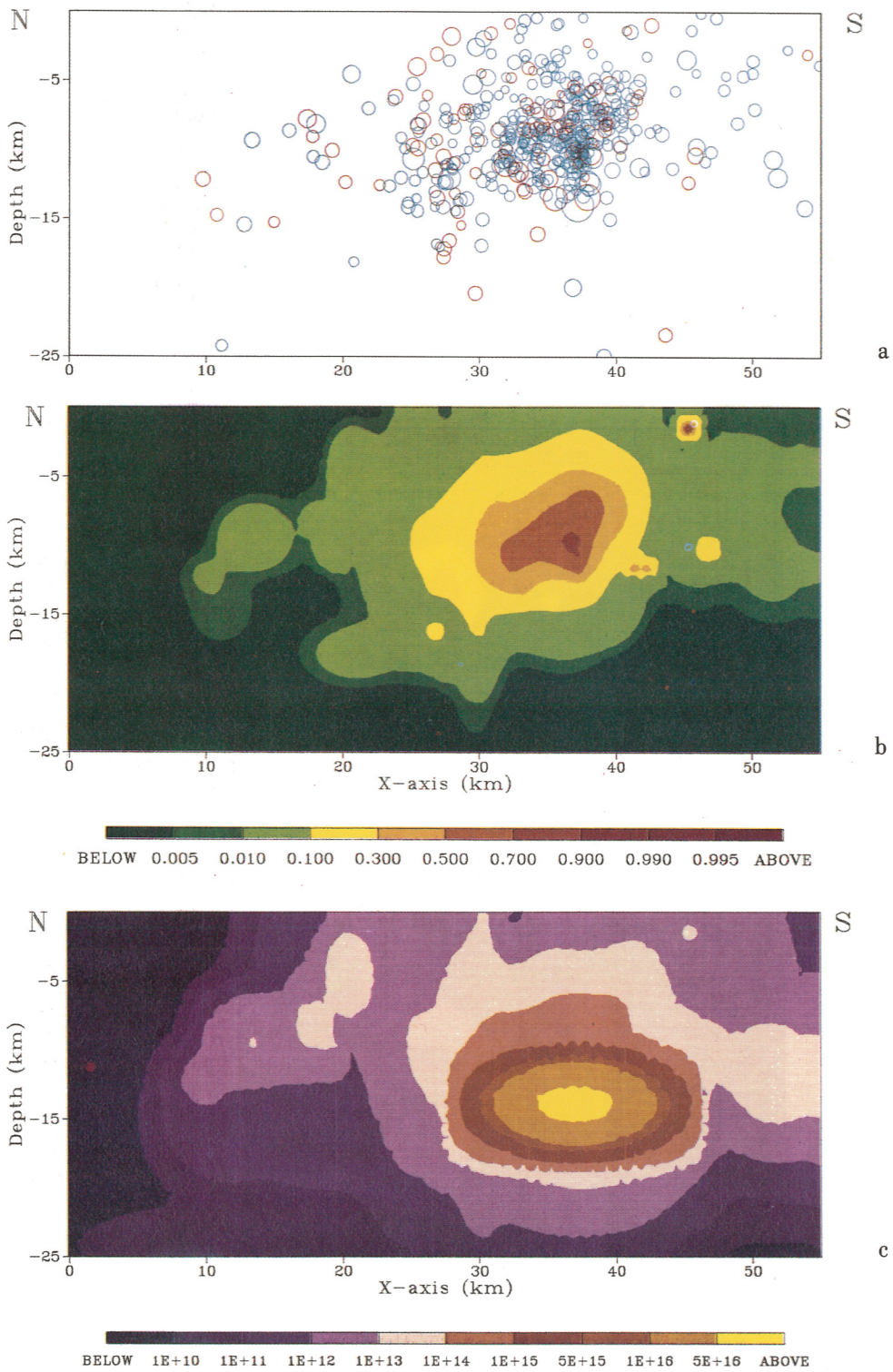

Fig. 11 - Maps of classical cross-section (a), *HP* distribution (b), and *ED* distribution (c) for Section 4. The coordinates of the extremes are 12.89 E - 46.64 N (the left corner), 12.98 E- 46.16 N (the right).

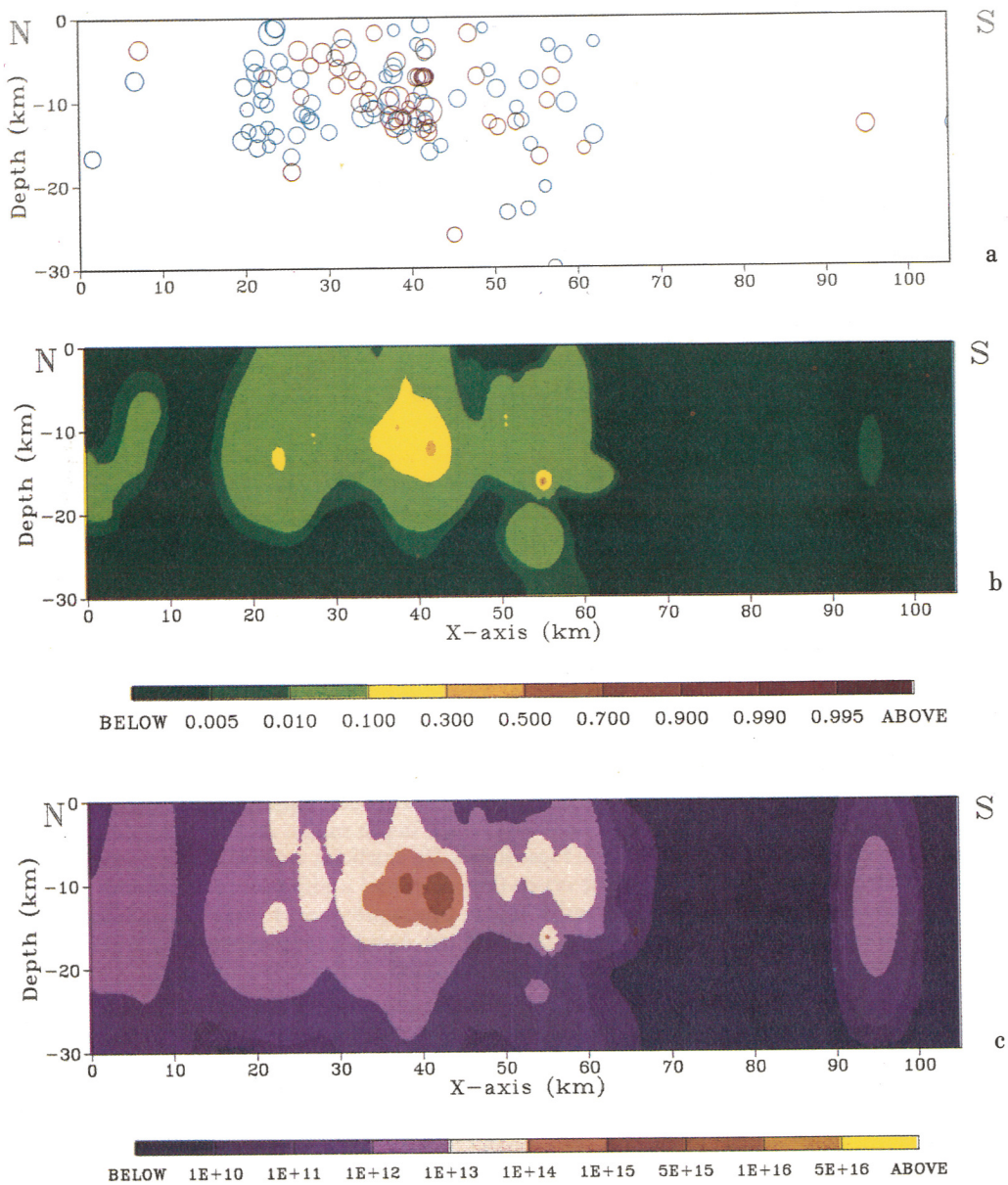

Fig. 12 - Maps of classical cross-section (a), *HP* distribution (b), and *ED* distribution (c) for Section 5. The coordinates of the extremes are 12.63 E - 46.68 N (the left corner), 12.88 E- 45.71 N (the right).

where some important vertical surficial faults are mapped. In Fig. 10b, the geometries found in Sections 1 and 2 survive, even if the most important maximum, with a mainly vertical development, is centred at 30-35 km on the X-axis. The time evolution analysis presented in Fig. 6 refers to Section 3 also, and it demonstrates that until 1987 the activity (Fig. 6a and b) was distributed with identical patterns, very similar to Sections 1 and 2, while the ultimate, quite energetic seismic crisis activated different structures. The new vertical geometry does not truncate the older pattern dipping north: a small elongation of the maximum on the vertical axis is certainly due to inaccuracies in depth determination.

Section 4 (Fig. 11a and Fig. 13 in Slejko et al., 1989a) is dominated by the strong 5.2 magnitude earthquake located at greater depth than the mean seismicity. Further relevant quakes occurred in the same area. Only a general northward deepening of the *HP* is clear (Fig. 11b). In the energy analysis, a strong maximum again swamps most of the possible information (Fig. 11c).

Finally, Section 5 illustrates the exit from the most important seismic zone and the few foci seem to be connected to discontinuities in the basement (depth greater than 10 km, in Fig. 12a and Fig. 14 in Slejko et al., 1989a). Although the thickness of the section in the computation is greater, nearly the whole section has a very low probability (less than 0.3) of having been the focus of at least one hypocenter (Fig.12b), making the *ED* maxima of Fig. 12c of low importance.

CONCLUSIONS

General remarks

The proposed methodology has the notable advantage over the classical representations of showing the actual space distribution of a probabilistic quantity without considering any a priori knowledge. In such a way, the detection of seismogenic structures can be automatically performed by simply analyzing the value of the maxima on differently oriented vertical cross-sections. Although the construction of the *HP* map is, at present, rather time consumming even on large computers, the simplified *HD* representation gives more easily obtained quite similar information.

Remarks on the application to the Friuli area

Applying the probabilistic method to an extensively studied area like Friuli has shown that the main results previously obtained by integrated analyses (Slejko et al., 1989a) come out easily, and further evidence arises. In brief, gently northward dipping structures under the piedmont belt, which are mainly active in the 7-12 km depth range, and vertical, less seismic, northern structures clearly appear (e.g. Figs. 8 and 9). Surficial vertical structures express a seismogenic character during particular crises (Fig. 9b), and a different inclination of the dipping planes is suggested by the high and medium probability areas (Fig. 10b). Some of the above ideas had already been formulated, but were not strongly supported by the foci distribution (part (a) of Figs. 8 to 12) alone, and more detailed analysis was required.

Some further information can sometimes be added to the *HP/ED* maps to support the seismotectonic interpretation; an example is the case of the slip vectors of the focal mechanisms (see the preliminary sketch in Peruzza et al., 1990b) which emphasize the dip of the breaking segments, and which are marked by *HP/ED* peaks in the seismogenic structures.

Acknowledgements. Many thanks are due to Chiara Molina, Politecnico of Milano, and to Paolo Scandone, University of Pisa, for reading and commenting the paper. The present research was done in the framework of activities supported by grants from the "Gruppo Nazionale per la Difesa dai Terremoti" of the "Consiglio Nazionale delle Ricerche".

REFERENCES

Cramer H.; 1955: *The elements of probability theory and some of its applications.* Robert Krieger Publishing Company, New York, 281 pp.

Lahr J.C.; 1979: *Hypoellipse: a computer program for determining local earthquake hypocentral parameters, magnitude and first motion pattern.* U.S.G.S. Open File Report 79-431, Menlo Park, 223 pp.

Lee W.H.K. and Lahr J.C.; 1975: *Hypo 71 (revised): a computer program for determining hypocenter, magnitude and first motion pattern of local earthquakes.* U.S.G.S. Open File Report 75-311, Menlo Park, 113 pp.

OGS; 1977-1981: *Bollettino della Rete Sismologica del Friuli-Venezia Giulia.* OGS, Trieste.

OGS; 1982-1989: *Bollettino della Rete Sismometrica dell'Italia Nord-Orientale.* OGS, Trieste.

Papoulis A.; 1977: *Probabilità, variabili aleatorie e processi stocastici.* Boringhieri, Torino, 600 pp.

Peruzza L., Padoan G., Rebez A. and Slejko D.; 1990a: *New methods in evaluating the seismicity along cross-sections.* In: ESC 22nd General Assembly: programme and abstracts, p. 172.

Peruzza L., Padoan G., Rebez A. e Slejko D.; 1990b: *Parametri per la valutazione di strutture sismogenetiche dedotti dalla sismicità regionale attuale.* In: Atti 9° Convegno Annuale GNGTS, ESA, Roma, in press.

Richter C.F.; 1958: *Elementary seismology.* Freeman and Co., San Francisco, 768 pp.

Riznichenko Y. V.; 1959: *On quantitative determination and mapping of seismic activity.* Ann. Geof., **12**, 227 - 237.

Slejko D., Carulli G.B., Carraro F., Castaldini D., Cavallin A., Doglioni C., Iliceto V., Nicolich R., Rebez A., Semenza E., Zanferrari A. e Zanolla C.; 1987: *Modello sismotettonico dell'Italia Nord-Orientale.* C.N.R. G.N.D.T. Rendiconto n. 1, Ricci, Trieste, 83 pp.

Slejko D., Carulli G.B., Nicolich R., Rebez A., Zanferrari A., Cavallin A., Doglioni C., Carraro F., Castaldini D., Iliceto V., Semenza E. and Zanolla C.; 1989a: *Seismotectonics of the eastern Southern-Alps: a review.* Boll. Geof. Teor. Appl., **31**, 109-136.

Slejko D., Peruzza L. e Iliceto V.; 1989b: *Orizzonti sismogenetici in Italia nord - orientale.* In: Atti 8° Convegno Annuale GNGTS, ESA, Roma, 35-40.